1.55 µm InP-based Short-Cavity-VCSELs with Enhanced Modulation-Bandwidth of 15 GHz

M. Müller[1], W. Hofmann[2], G. Böhm[1], J. Rosskopf[3], E. Rönneberg[3], M. Ortsiefer[3], M. C. Amann[1]

[1] Walter Schottky Institut, Technische Univeristät München, Am Coulombwall 3, D-85748 Garching, Germany, michael.mueller@wsi.tum.de

[2] Dept. of Electrical Engineering and Computer Sciences, University of California at Berkeley, CA 94720, USA

[3] VERTILAS GmbH, Lichtenbergstr. 8, D-85748 Garching, Germany

Abstract *InP-based burried tunnel junction VCSELs incorporating a novel short-cavity design are presented. These devices show record-high modulation-bandwidths in excess of 15 GHz together with greatly enhanced intrinsic resonance-frequencies. Intrinsic damping is improved due to reduced photon-lifetime.*

Introduction

Vertical-Cavity Surface-Emitting Lasers (VCSELs) operating at bit-rates up to 25 Gb/s have been presented recently[1]. Emitting in the near infrared waveband around 850 nm, these lasers can only be used for short transmission-distances. Therefore, great efforts in developing long-wavelength, high-speed VCSELs have been made - with steady improvement[2-4]. Promising results and record-high modulation bandwidths have especially been shown for long-wavelength VCSELs with buried tunnel junction (BTJ)[5].

With 100G Ethernet standards in discussion, parallel approaches of 8 x 12.5 Gb/s, 6 x 17 Gb/s, or 4 x 25 Gb/s are desirable, favoring higher serial bandwidth due to cost issues. Therefore, the modulation bandwidth of the laser source has to be further improved. For data transmission at 12.5 Gb/s, 17 Gb/s, and 25 Gb/s a respective modulation bandwidth of 10 GHz, 13 GHz, and 19 GHz is required[3].

In this paper we present a high-speed long-wavelength BTJ VCSELs incorporating new short-cavity (SC) design. The effect of a shorter cavity on the bandwidth is discussed and demonstrated.

Device Structure and DC-Characteristics

The high-speed 1.55 µm VCSEL structure is a completely novel structure based on the device reported earlier[3]. The schematic layout of the laser chip in Fig. 1 shows the implementation of a second dielectric AlF_3/ZnS top-mirror replacing the epitaxially grown one from Ref. 3. Epitaxial mirrors at these wavelength do not only show poor thermal conductivity, but also suffer from low refractive index contrast resulting in large penetration depths. Consequently, the effective cavity length is greatly reduced with the novel dielectric out-coupling mirror As will be shown, both, the reduced cavity length and the use of benzocyclobutene (BCB) as passivation with low dielectric constant are crucial for high-speed operation. Moreover, the substitution of the 8 µm thick arsenic-based epitaxial mirror is favourable in concerns of fabrication costs and Green-IT.

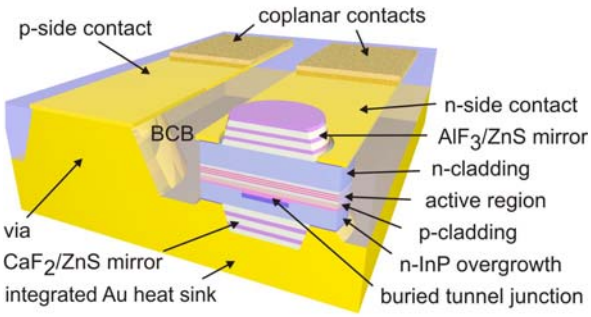

Fig. 1: Schematic cross-section of a high-speed 1.55 µm InP-based BTJ VCSEL with dielectric top- & bottom-mirror. The device is mounted epi-side down on an electroplated gold heat sink. The InP substrate is removed during manufacturing. Both *n*- and *p*-contact can be accessed on top. Contact-pad capacitances are minimized.

Furthermore, the dielectric top-mirror allows the application of an intra-cavity contact improving the heat flow from the active region to the contact-pads due to the high heat-conductivity of the InP heat- and current-spreader. In order to enhance high-speed operation and (differential) gain, the active region consists of 7 heavily compressive-strained quantum wells. The pseudomorphic strain was tailored to be 2.5% which is close to the critical layer thickness. Therefore, low threshold currents and high relaxation oscillation frequencies are expected. The doping-level of the InP-overgrowth has been lowered in order to reduce the parasitic capacitance of the space charge region which strongly influences the modulation behavior[3]. The hybrid back-mirror of the lasers consist of 3.5 pairs of lossless CaF_2/ZnS and a gold heat sink, facilitating very high reflectivities (>99.9%) and improved heat management at the same time.

Fig. 2 shows the *LIV*-characteristics of a typical device. For a current aperture of 5 µm, the maximum optical output power is 2.0 mW at room-temperature and still exceeds 0.8 mW at 65°C. Threshold currents and voltages are as low as 1 mA and 1 V, respectively. The spectrum, depicted in the inset of Fig. 2, shows single-mode operation with a side mode suppression ratio of more than 40 dB over the entire temperature range.

978-3-8007-3173-2

Modulation Performance

From rate-equation analysis one finds that the relaxation-resonance frequency scales with the inverted square root of the cavity-volume[6]. Therefore, our new short-cavity design, with the effective cavity length reduced by more than 30% compared to our earlier but otherwise identical design[3], should facilitate an increase of the relaxation-resonance frequency by 20%.

The small-signal modulation performance was verified on chip-level for various bias currents. The measurements were performed using a HP8510C vector-network analyzer with matched and calibrated photodiode. The chip was probed with a Cascade microprobe and calibration was done to the chip-plane with a Cascade calibration substrate. A signal-level of -6 dBm was chosen. In Fig. 3 scatters represent the measured S_{21}-data. Solid lines represent fits of the squared three-pole filter function

$$H(f) = \eta_{d,L}\eta_{d,PD} \cdot \frac{f_R^2}{f_R^2 + j\frac{\gamma}{2\pi}f - f^2} \cdot \frac{1}{1 + j\frac{f}{f_P}} \qquad (1)$$

Thereby, f_R is the relaxation-resonance frequency, γ the intrinsic damping, and f_P the parasitic roll-off frequency.

Table 1 shows the values of these intrinsic parameters extracted from the fit. A maximum relaxation-resonance frequency of 14.1 GHz and a 3dB-cutoff frequency exceeding 15 GHz is observed for an applied bias-current of 9.9 mA. For even higher currents increased intrinsic and thermal damping dominates the modulation behaviour. From Tab.1 the *K*-factor and the damping offset are determined to be as low as 0.17 ns and $22 \cdot 10^9\ s^{-1}$, respectively. This improved damping behaviour is caused by the reduced cavity length which is also a measure for the photon-life-time. Since the *K*-factor scales linearly with the photon-lifetime, we should expect a reduction by at least 30% in comparison to the *K*-factor of 0.3 ns in our earlier design with 30% longer cavity[3]. For the device presented here the *K*-factor (0.17 ns) shows an even stronger relative reduction.

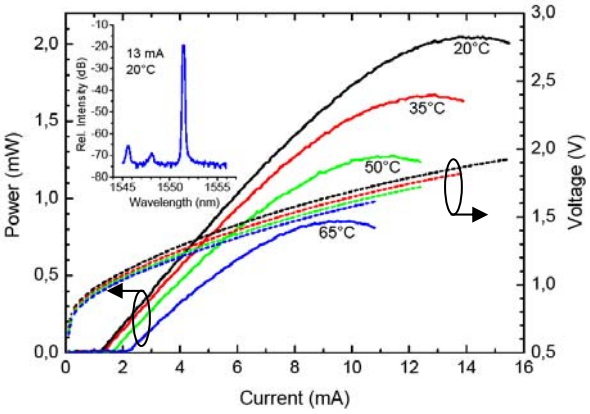

Fig. 2: *LIV*-characteristics of high-speed 1.55 µm VCSEL at different temperatures. Single-mode spectrum is depicted as inset. The device's aperture is 5 µm.

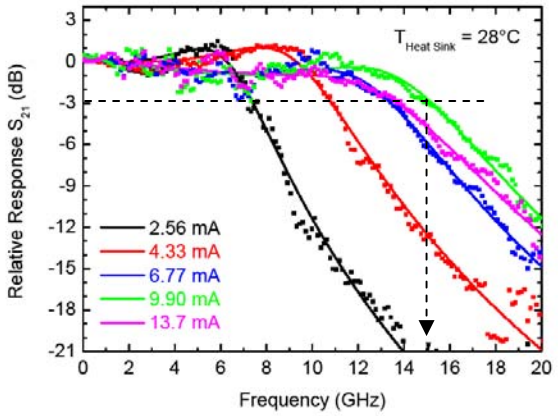

Fig. 3: Relative response S_{21} versus modulation frequency for various bias-currents applied to a 1.55 µm SC-VCSEL at 28°C. Maximum 3dB-cutoff frequency is indicated.

I (mA)	f_R (GHz)	f_P (GHz)	γ ($10^9 s^{-1}$)
2.56	6.5	5.2	26.6
4.33	9.4	7.1	36.6
6.77	12.6	6.7	46.4
9.90	14.1	7.3	49.1
13.7	13.6	7.9	59.9

Tab. 1: Relaxation-resonance frequency, parasitic roll-off frequency, and intrinsic damping determined from the fit of equation (1) to the respective *S*21-data in Fig. 3 for various bias-currents.

Conclusion

In this paper we have presented 1.55 µm BTJ-VCSELs with improved high-speed performance due to the application of a novel short-cavity design. A record-high small-signal modulation bandwidth in excess of 15 GHz is achieved up to 28°C, originating from improved intrinsic damping and increased relaxation-resonance frequencies. Therefore, data-rates of 17 Gb/s for 100G Ethernet are feasible with these devices.

References

1 P. Westbergh et al., Electron. Lett., vol. 44, no. 15, pp. 907-908, (2008).
2 F. Hopfer et al., IEEE J. Sel. Top. Quant. Electron., vol. 13, no. 5, pp. 1302-1308, (2007).
3 W. Hofmann et al., IEEE Phot. Tech. Lett., vol. 20, no. 11, (2009).
4 N. Nishiyama et.al., OFC/NFOEC, OMK4, pp. 1-3, (2007).
5 M.C. Amann et al., IEEE J. Sel. Top. Quant. Electron., to be published in 2009.
6 L.A. Coldren et al., *Diode Lasers and Photonic Integrated Circuits*, John Wiley & Sons, pp 199-204, (2009).